JOURNAL OF NANO- AND ELECTRONIC PHYSICS
Vol. **10** No 5, 05020(6pp) (2018)

ЖУРНАЛ НАНО- ТА ЕЛЕКТРОННОЇ ФІЗИКИ
Том **10** № 5, 05020(6cc) (2018)

Fabrication of Room Temperature NO_2 Gas Sensor based on Silver Nanoparticles-Decorated Carbon Nanotubes

Waleed Kh. Mahmood, Asama N. Naje

Baghdad University, College of Science, Physics Department, Baghdad, Iraq

(Received 19 August 2018; revised manuscript received 20 October 2018; published online 29 October 2018)

Functionalized-single wall carbon nanotubes (F-SWCNTs) were easily and efficiently decorated with Ag Nanoparticles. The sensor device consisted of a film of sensitive material (F-SWCNTs) and (F-SWCNTs/Ag NPs) deposited by drop coating on n-type porous silicon substrate. The two sensors show high sensitivity to NO_2 gas at different temperatures. Test results demonstrated that the (F-SWCNTs/Ag NPs) have a better performance than (F-SWCNTs). The F-SWCNTs gas sensor shows high sensitivity (36 %) at RT with response time 11 sec, whereas F-SWCNTs/Ag NPs gas sensor shows better sensitivity (150.5 %) at RT with response time 8 sec. The device shows a very reproducible sensor performance, with high repeatability, full recovery and efficient response. The improvement in the detection of some specific gases (NO_2) using Ag-functionalized nanotubes is explained.

Keywords: Functionalized-SWCNTs, NO_2 gas, Porous Silicon, Sensitivity, Silver NPs, Response time, Fermi level, Room temperature, Chemical reduction.

DOI: 10.21272/jnep.10(5).05020 PACS numbers: 07.07.Df, 61.46.Df, 78.67.Bf

1. INTRODUCTION

Carbon nanotubes (CNTs) are active materials both as a guideline of basic physical properties in a one-dimensional nanosystem and for a wide type of nanotechnology applications [1]. Specifically, due to their high surface to volume ratio and being described by a conductance that can be readily perturbed by interaction with gas molecules, CNTs are favorable candidates as elements for the highly sensitive gas-sensing system [2]. However, the response of carbon nanotubes to gases is low and hardly selective since the carbon hexagonal arrangement is held together by strong sp^2 bonds characterized by a weak chemical reactivity with the molecular environment. Accordingly, the functionalization of the CNT sidewalls is compulsory to enhance both the sensitivity and the selectivity of carbon nanotubes based gas sensors [3]. Specifically, functionalization with metal nanoparticles (NPs) can prompt profoundly delicate and selective gas sensors because of the remarkably catalytic properties of metal NPs [4], as already suggested by several experimental theoretical and combined works [5-7]. In spite of the fact that the sensing capacity of CNTs decorated with metal NPs depends on the massive chemical reactivity of the cluster surface, the entire CNT-NP system acts as the sensing unit of the device. In fact, the interaction with gases effects in an electronic charge exchange between the molecule and the CNT-NP sensor, which influences the situation of the Fermi energy and, subsequently, the conductivity of the sensing unit. The adsorption of an additional electron origination from molecules displaying a donor character will prompt an increase of the resistance. Similarly, the interaction with molecules displaying an acceptor character will prompt a decrease in the resistance. Indeed, functionalization of CNTs with metal nanoparticles can be exploited to enhance the sensor selectivity, since various metals will exhibit different re-activities toward various molecules. Subsequently, a gas sensor gadget can be fabricated by decorated with a different kind of metallic NPs [8]. These days, Ag NPs has increase gigantic prominence in the world in the field of sensors as a result of exceptional hugeness optical, electronic and chemical properties [9]. The present work study the sensing performance of the CNTs NO_2 gas sensor by using (F-SWCNTs and F-SWCNTs/Ag NPs) and make comparisons between them to get the best performance.

2. EXPERIMETAL

2.1 Preparation of Porous Silicon (Psi)

In this work, 2×2 cm^2 dimensions primary *n*-type silicon wafer substrates were thoroughly cleaned to decontaminate their surface from any available stains and dirt. A porous silicon layer (PS) was prepared via electrochemical etching. This process was carried out by immersing the samples in HF acid of 40 % concentration mixed with ethanol in (1:1) ratio in a Teflon beaker. The applied current density was 20 mA/cm^2, and the typical electrochemical-etching time was chosen to be about 20 minutes.

2.2 Preparation of Silver Nanoparticles

Silver NPs were synthesized by the chemical reduction (cold method). At first, $AgNO_3$ had been prepared by dissolving 0.018 g of $AgNO_3$ in 100 mL distilled water. Then, $NaBH_4$ prepared by dissolving 0.020 g of $NaBH_4$ in 250 mL distilled water. By adding 30 mL of $NaBH_4$ to an Erlenmeyer flask, we put a magnetic stir bar and placed the flask in an ice bath on a stir plate. The liquid had been stirred and cooled for about 20 minutes. Then, dropped 2 mL of $AgNO_3$ into the stirring $NaBH_4$ solution at approximately 1 drop per second. The liquid is starting to seem as yellow after two minutes which indicates to creation silver nanoparticle. The chemical reaction is:

$$AgNO_3 + NaBH_4 \rightarrow Ag + H_2 + B_2H_6 + NaNO_3 \quad (1)$$

Finally, we dissolved 0.3 % PVP solution (0.1 g of PVP) in 33 mL distilled water. Then many drops of PVP had been added as a preventing agent the liquid of Ag NPs.

2.3 Decoration of F-SWCNTs with AgNPs

To prepare CNT sample, 0.01 g of CNT was dispersed in Dimethylformamide (DMF). A magnetic stirrer was incorporated for this purpose for 15 minutes, followed by 1-hour sonication. The decoration of Ag-NPs on the COOH-functionalized SWCNTs was conducted. After the formation of silver nanoparticles occurred, 200 μL of functionalized SWCNTs were added with 100 μL of the Ag NPs stirred for 4 h and followed by 1-hour sonication. The obtained solution was used for film deposition on porous silicon by the drop casting method.

3. RESULTS AND DISCUSSION

3.1 Structural and Morphological Characteristics

The surface morphology and topography of the porous silicon layer observed from the AFM micrograph is shown in Fig. 1. It is observed that nanoporous silicon had a regular distribution and homogeneous porous and the average surface roughness was 6.93 nm, 31.96 nm high and average porous size was 77.47 nm.

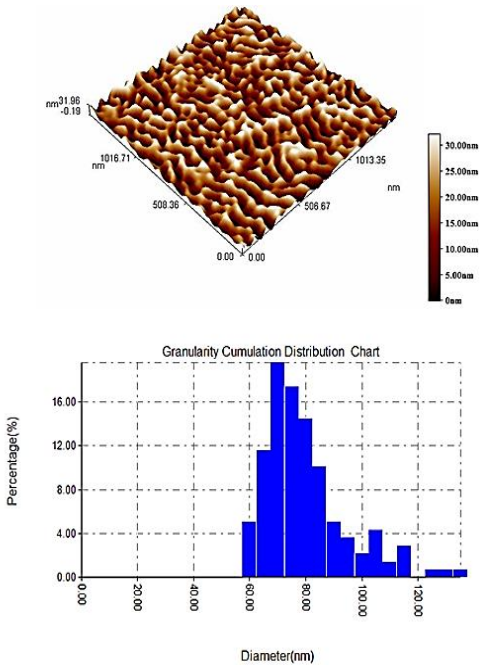

Fig. 1 – The AFM for porous silicon layer of 20 minutes etching time

The Atomic Force Microscope (AFM) of the SWCNTs/AgNPs on PS is shown in Fig. 2, the surface morphology of the SWCNTs/AgNPs film had a good a uniform surface with regular distribution of the SWCNTs/Ag nanoparticles with the average surface roughness was 0.63 nm, 2.62 nm high and average porous size 69.08 nm.

In Fig. 3 long nanotubes with large agglomerates and closely packed CNTs can be seen.

In the Fig. 4 the SEM image of Ag NPs shows the spherical clustered and the luminous of Ag NPs.

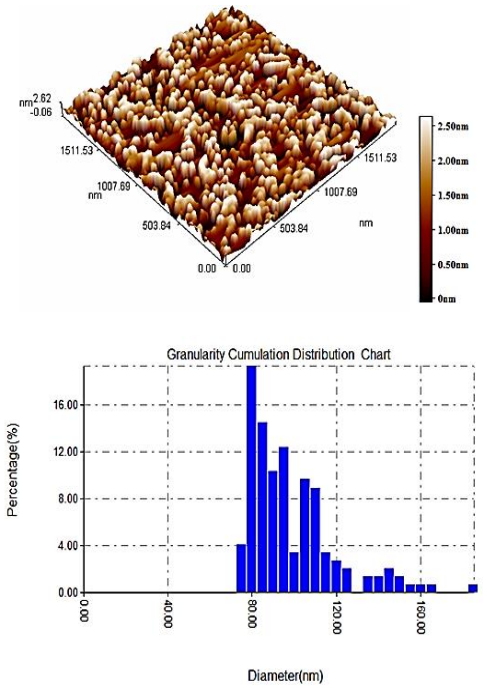

Fig. 2 – The AFM for the SWCNTs/AgNPs deposited on PS nanosurface

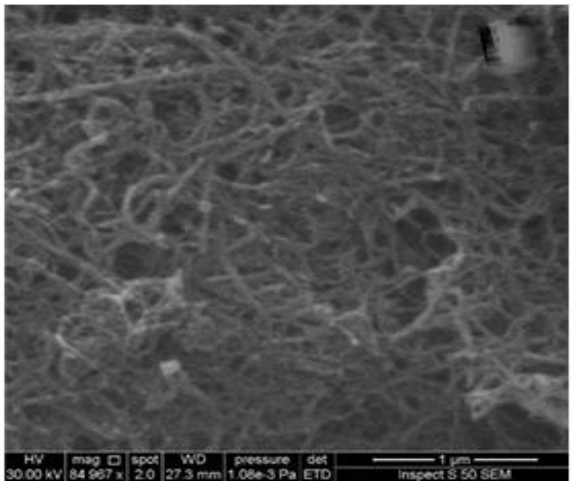

Fig. 3 – SEM images of SWCNTs film

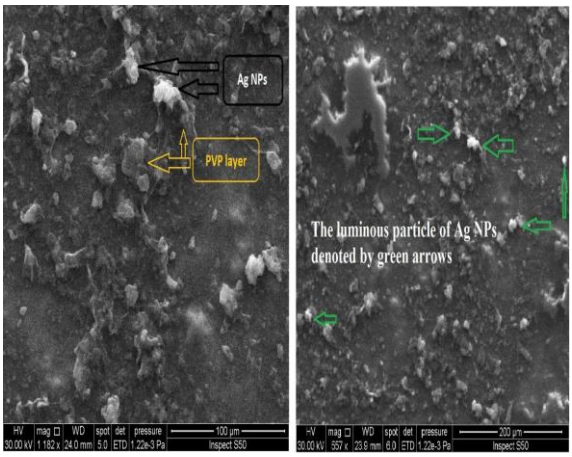

Fig. 4 – SEM images of AgNPs

From the XRD diffraction pattern of Ag nanoparticles, all diffraction peaks of sample correspond to the characteristic face centered cubic structure of Ag nanoparticles ($a = 0.407$ nm) [9]. The average particle size of Ag nanoparticles is found to be 22 nm using Scherrer equation [11]. Diffraction pattern corresponding to impurities is found to be absent. This proves that pure Ag nanoparticles were as synthesized. The Ag NPs have a cubic polycrystalline structure with peak positions which agree with the standard data get from PCPDFWIN (card no. 7440-22-4).

Table 1 shows the full width half maxima, *d*-spacing, Miller indices and crystalline size of Ag nanoparticles.

Table 1 – The crystalline Size of the Prepared Ag Nanoparticles as Estimated via the Scherrer Formula

2Theta(degree)	Cos θ	β (degree)	Crystalline size (D) nm	Lattice parameter a (Å)	*d*-spacing nm	(*hkl*)
38	0.987	0.24	33.9	4.070	0.235	(111)
44	0.927	0.48	17.26	4.068	0.203	(200)
64	0.848	0.56	16.925	4.073	0.144	(220)

X- ray diffraction was used to study the crystal structure of SWCNTs powder. The diffraction pattern SWCNTs appeared at 2θ of 26° and 44.5°. The 2θ peaks corresponds to (002) and (100) reflection planes or also known as interlayer spacing between adjacent graphite layers and these peaks reflect hexagonal structure. This is in agreement with results reported by other researchers [12].

Table 2 shows the grain size of SWCNTs from X-ray diffraction patteren and by using Scherer's formula Eq formula [11].

Table 2 – Crystalline size of the CNTs powder as estimated via the Scherer formula

CNT type	2Theta (degree)	Cos θ	β (rad)	Crystalline size *D* (nm)	*hkl*	Average crystalline size (nm)
SWCNTs	26	0.974	0.122	1.16	002	1.325
	44.5	0.925	0.104	1.49	100	

Analysis of Energy Dispersive X-rays (EDX) by Bruker Nano GmbH, Germany SEM. The EDX gives a real approved forming the Ag NPs in the colloidal with concentration reach 1.6 mg per 200 ml. And the EDX spectrum of SWCNTs Thin films were deposited on n-type PS wafers. The EDX trace confirms qualitatively the existence of the carbon (C) and silicon (Si) elements, where the thickness of SWCNTs is 0.112 μm.

UV-vis absorption spectrum of the prepared Ag NPs are measured using Shimadzu UV-1800 spectrophotometer, covering a range from (190-1100) nm. The scanning range of the Ag nanoparticles absorption was (300-900) nm using distilled water for Ag NPs as a reference sample. Fig. 5 shows the UV-Visible absorption spectra of Ag nanoparticles colloidal as a function of wavelength. The optical properties of silver nanoparticles are strongly affected by the Local Surface Plasmon Resonance (LSPR). The UV-Visible absorption spectra of Ag NPs in Fig. 5 have a knee in the UV region at 272 nm, and flat, broadband was narrower of small absorption peak in the visible range of 426 nm. The color of the prepared silver nanoparticles is yellow as shown in Fig. 10.

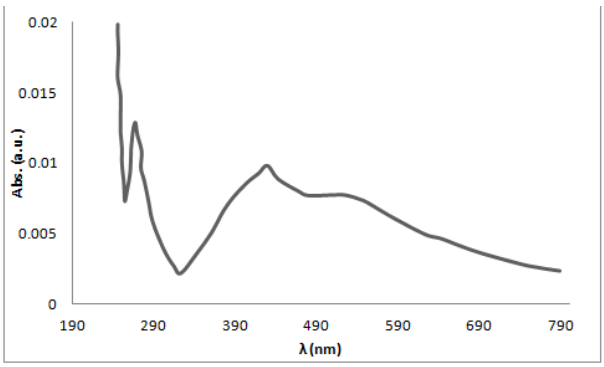

Fig. 5 – Absorption peak of silver nanoparticles at 426 nm

Fig. 6 – Silver NPs colloidal

FTIR studies have been performed in the range 400 to 4000 cm^{-1} for the identification of the SWCNTs/AgNPs deposited on quartz substrates. Fig. 7 shows the FTIR spectrum for SWCNTs/AgNPs. For SWCNTs, the peaks are observed at 3481, 3440, 3367 and 1623 cm^{-1} confirming the presence of the O–H stretching band and the COOH asymmetric stretching band, and the peaks appearing in the range of 1512.09-1400 cm^{-1} are attributed to the C–C stretch. Moreover, the peak at 1335-1000 cm^{-1} confirming the presence of the C-O stretch, as shown in fig. 7 [12]. For SWCNT-AgNPs, the peaks at 1625.82 and 668.05 cm^{-1} are corresponding to Ag–O stretching and deformation vibration, respectively. The metal-oxygen frequencies observed for the respective metal oxides are in accordance with literature values [13].

3.2 Gas-sensing Properties

The sensor response (S) is defined as the ratio of the change in resistance ($R_g - R_a$) upon exposure to target analyte to the resistance (R_a) of the sensor in air.

$$S = \left| \frac{R_{air} - R_{gas}}{R_{gas}} \right| \times 100\%, \quad (2)$$

where, R_g and R_a are the resistances of the sensor in the presence of NO_2 and in air respectively. The response time and recovery time were calculated as the time taken for the sensor to attain 90 % of total re-

sistance change (t_{90}) from its initial resistance.

In Fig. 8 and 9, shows the variation of resistance as a function of time. Experimental results indicated an increase in conductance of CNTs and CNTs/AgNPs when exposed to oxidizing gases like NO_2. This behavior may be attributed to the charge transfer occurring from CNTs and CNTs/AgNPs to NO_2 because of its highly oxidizing nature.

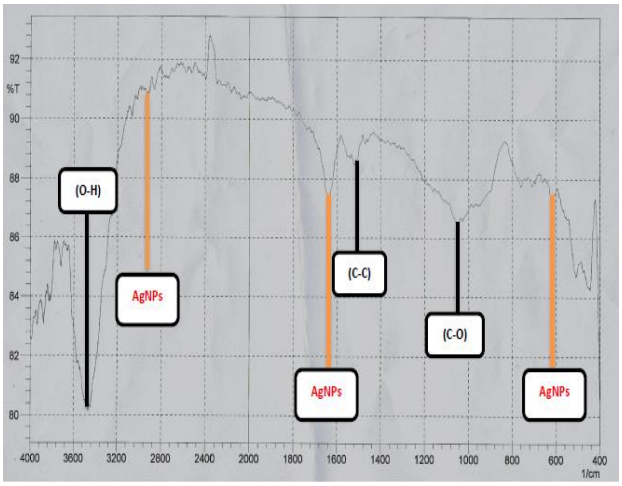

Fig. 7 – FTIR of (F-SWCNTs and F-SWCNTs/AgNPs)

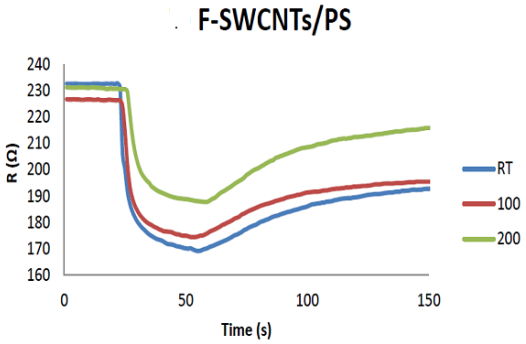

Fig. 8 – Resistance-time variation of CNTs sensor time at RT, 100 °C and 200 °C testing temperature upon exposure to NO_2 gas for F-SWCNTs

Table 3 shows the sensitivity, response and recovery time for F-SWCNTs/PS and F-SWCNTs/AgNPs/PS upon exposure to the NO_2 gas.

The response time of the F-SWCNTs gas sensor decreases and increases for F-SWCNTs/AgNPs with increasing the operating temperature, with the shortest response and recovery times being at about 8 s and 15 s, respectively at RT for F-SWCNTs/AgNPs , and 8 s and 13s at 100 °C for F-SWCNTs, as shown in Fig. 14 and 15.

Fig. 10 shows the sensitivity *S*% of F-SWCNTs and F-SWCNTs/AgNPs deposited on Porous Silicon to NO_2 gas. The test performed at 1:1, NO_2: air gas mixing ratio. It is shown that the sensitivity decreased with increasing the operating temperature T. The maximum sensitivity of *F-SWCNTs*/PS of 36 % was obtained at RT testing temperature after which it began to drop with increasing T. While the sensitivity of F-SWCNT/AgNPs/PS of 150.5 % was obtained at RT °C testing temperature after which it began to drop with increasing *T*.

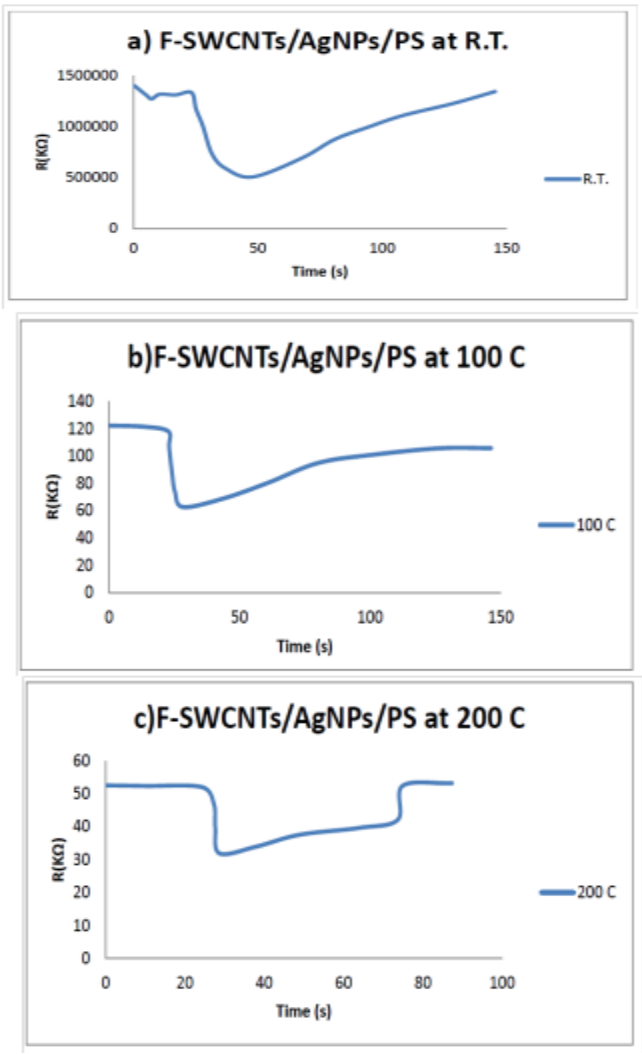

Fig. 9 – Resistance-time variation of CNTs sensor upon exposure to NO_2 gas for F-SWCNTs/AgNPs time at 200 °C testing temperature a) R.T., b) 100 °C , c) 200 °C

Table 3 – The sensitivity, Response and Recovery time of F-SWCNTs/PS and F-SWCNTs/AgNPs/PS thin film upon exposure to NO_2 gas at different operating temperature

Type	*T* (°C)	*S* %	t_s (s)	t_c (s)
F-SWCNTs/AgNPs/PS	RT	150.5	8	15
	100	96.6	22	23
	200	69.1	16	19
F-SWCNTs/PS	*T* (°C)	*S* %	t_s (s)	t_c (s)
	RT	36	11	26
	100	29.7	8	13
	200	23	14	18

The increase of sensitivity of F-SWCNTs and F-SWCNTs/AgNPs can be attributed to deposits of CNTs and CNTs/AgNPs on porous silicon because porous silicon will increase the surface area of interaction between (CNTs, and CNTs/AgNPs) and NO_2 gas. Also, using functionalized SWCNTs will provide open side wall due to oxidative damage to the nanotube framework by strong acids, which leave holes functionalized with oxygenated functional groups (-COOH). This treatment of CNTs with strong acids tends to open the-

se tubes, which increase the adsorption of the gas in the CNTs wall and increase the sensitivity. Finally, adding AgNPs also will increase the surface area and favor the adsorption of the gas, and this will allow to great interaction between the gas molecules and the surface. In this case, the nanotubes still acts as a transducer system, while the metal NPs on the surface became the sensing part of the device.

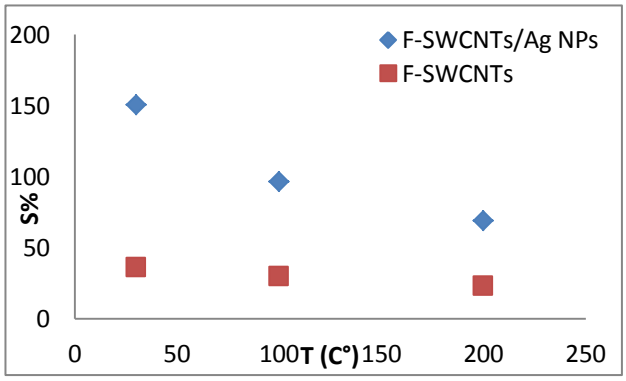

Fig. 10 – Sensitivity of F-SWCNTs and F-SWCNTs/AgNPs thin film at various testing temperatures upon exposure to 1:1, NO_2 gas:air

As a general overview of the results, sensor resistance decreases with increasing concentrations of NO_2, which is an electron acceptor. The response of the CNTs sensor to NO_2 is in agreement with trends reported elsewhere [14]. Accordingly, carbon nanomaterials are very suitable for detecting the NO_2 gas by measuring the changes in the electrical conductance. Specifically, carbon nanomaterials have higher carrier mobility and they can be extremely sensitive toward changes in their local environment [15]. The composite material offers higher sensitivity and signal response to NO_2 gas than pristine SWCNTs. In order to explain the results, the chemical nature of the NO_2 molecule is considered. Recent experimental results show that the electrical conductance of an individual semiconducting single walled tube strongly increases upon NO_2 gas exposure and that the NO_2 is identified as an electron acceptor. In light of the present work, it is reasonable to propose that this behavior in the nanotubes film is also due to adsorbed NO_2 in the tube wall. According to the calculations, a possible interpretation of the electrical response of CNT films to NO_2 gas could be explained in terms of the physical absorption of this molecule. NO_2 has an unpaired electron and is known as a strong oxidizer. Upon NO_2 adsorption, a charge transfer is likely to occur from the CNTs to the NO_2 due to the electron–acceptor character of NO_2 molecules. The electrical response of the CNTs indicates that there is a charge transfer between the test gas and sensing element, and hence, that the physisorption of gases in the nanotubes is the dominant sensing mechanism. The effects of Ag NPs are as follows. First, Ag NPs contribute significantly to improving the conductivity of CNTs, leading to better sensing behavior. Second, the NO_2 gas was distributed over the CNTs sheets by Ag NPs acting as a catalyst, with improved adsorption and desorption of NO_2 gas molecules on Ag NP surfaces owing to the highly catalytic or conductive nature of Ag. Thus, the number of electrons attracted to NO_2 (electron acceptor) increases. Third, electron transfer from the defect states (sp^3-hybridized carbons) to Ag NPs not only increases the resonant electron density, but also creates energetic electrons in high-energy states. The role of Ag NPs as electron mediators further facilitates electron transfer from CNTs to NO_2 molecules, as given in equations (3) and (4).

$$NO_2 + e^- \rightarrow NO^{-2} \quad (3)$$

$$NO_2 + O_2^- \rightarrow NO^- + O_2 \quad (4)$$

Therefore, the Ag NPs significantly decrease the electron density of the CNTs. As an important property of gas-sensing devices, the Ag NPs-CNTs device shows selectivity for NO_2 gas detection.

4. CONCLUSION

Comparative gas sensing property analysis of the F-SWCNT and F-SWCNTs/Ag NPs nanocomposite based gas sensors revealed excellent sensor performance for F-SWCNTs/Ag NPs nanocomposite based sensor compared to F-SWCNT for NO_2 which is attributed to the presence of AgNPs on the surface of SWCNT. Moreover, fast response and good reversibility were observed for the F-SWCNTs/AgNPs based sensor compared to the F-SWCNTs which can be mainly attributed to the enhanced charge transfer through metal NPs on F-SWCNTs. The F-SWCNTs/AgNPs nanocomposite was found to be highly selective towards NO_2 gas. The study explores the possibility of using F-SWCNTs/AgNPs based on, the low cost and low temperatures for the sensing of NO_2 gas. The sensor device (F-SWCNTs/AgNPs) has proved highly efficient in use as a sensor to detect NO_2 gas. And it could open prospects for development as a result that chemical sensor may reach the level of dealing with one molecule of gas and shorten the sensor response time. The sensor device in the present work approves a high accuracy and sensitivity, high level of selectivity, a short response and recovery time, low operating temperature and stability in performance.

REFERENCES

1. Zeila Zanolli, Radouane Leghrib, Alexandre Felten, Jean-Jacques Pireaux, Eduard Llobet, Jean-Christophe Charlier, *ACS Nano* **5**(6), 4592 (2011).
2. A. Goldoni, L. Petaccia, S. Lizzit, R. Larciprete, *J. Phys. Condens. Matter* **22**, 013001 (2010).
3. Ali Eatemadi, Hadis Daraee, Hamzeh Karimkhanloo, Mohammad Kouhi,Nosratollah Zarghami,Abolfazl Akbarzadeh, Mozhgan Abasi, Younes Hanifehpour, Sang Woo Joo, *Nanoscale Res. Lett.* **9**, 393 (2014).
4. Yong Jung Kwon, Han Gil Na, Sung Yong Kang, Sun-Woo Choi, Sang Sub Kim, Hyoun Woo Kim, *Sensor. Actuat. B* **227**, 157 (2016).
5. Eduardo Gracia-Espino, Bernabé Rebollo-Plata, Hugo Martínez-Gutiérrez, Emilio Muñoz-Sandoval, Florentino

López-Urías, Morinobu Endo, Humberto Terrones, Mauricio Terrones, *J. Sensor.* **2016**, Article ID 4319498 (2016).
6. R. Leghrib, A. Felten, F. Demoisson, F. Reniers, J.-J. Pireaux, E. Llobet, *Carbon*, **48**, 3477 (2010).
7. Q. Zhao, M. Nardelli, W. Lu, J. Bernholc, *Nano Lett.* **5**, 847 (2005).
8. J.-C. Charlier, *Nanotechnology* **20**, 375501 (2009).
9. Asama N. Naje, Waleed K. Mahmood, Rawa K. Ibrahim, *Iraqi J. Sci.* **58** No 4B, 2090 (2017).
10. T.R. Jensen, G.C. Schatz, V.R.P. an Duyne, *J. Phys. Chem. B* **103**, 2394 (1999).
11. D.P. Padiyan, A. Marikani, K.R. Murali, *Mater. Chem. Phys.* **78**, 51 (2003).
12. M. Chen, W. Oh, *Nanoscale Res. Lett.* **6**(1), 398 (2011).
13. G.-W. Lee, J. Kim, J. Yoon, J.S. Bae, B.C. Shin, I.S. Kim, W. Oh, M. Ree, *Thin Solid Films* **516**, 5781 (2008).
14. C.N.R. Rao, *Chemical Applications of Infrared Spectroscopy* (Academic Press: New York and London: 1963).
15. J.A. Misewich, R. Martel, Ph. Avouris, J.C. Tsang, S. Heinze, J. Tersoff, *Science* **300**, 783 (2003).
16. J. Li, Y. Lu, Q. Ye, M. Cinke, J. Han, M. Meyyappan, *Nano Lett.* **3**, 929 (2003).